

Relative stability and significance of dawsonite and aluminum minerals in geologic carbon sequestration

John P. Kaszuba,¹ Hari S. Viswanathan,² and J. William Carey²

Received 25 January 2011; revised 2 March 2011; accepted 8 March 2011; published 22 April 2011.

[1] Computer simulations predict dawsonite, $\text{NaAlCO}_3(\text{OH})_2$, will provide long-term mineral sequestration of anthropogenic CO_2 whereas dawsonite rarely occurs in nature or in laboratory experiments that emulate a carbon repository. Resolving this discrepancy is important to determining the significance of dawsonite mineralization to the long-term security of geologic carbon sequestration. This study is an equilibrium-based experimental and modeling evaluation of underlying causes for inconsistencies between predicted and observed dawsonite stability. Using established hydrothermal methods, 0.05 molal NaHCO_3 aqueous solution and synthetic dawsonite were reacted for 18.7 days (449.2 hours) at 50°C, 20 MPa. Temperature was increased to 75°C and the experiment continued for an additional 12.3 days (295.1 hours). Incongruent dissolution yielded a dawsonite-gibbsite-nordstrandite assemblage. Geochemical simulations using Geochemist's Workbench and the resident database thermo.com.V8.R6⁺ incorrectly predicted a dawsonite-diaspore assemblage and underestimated dissolved aluminum by roughly 100 times. Higher aqueous aluminum concentrations in the experiment suggest that dawsonite or diaspore is less stable than predicted. Simulations employing an alternate database, thermo.dat, correctly predict dawsonite and dawsonite-gibbsite assemblages at 50 and 75°C, respectively, although dissolved aluminum concentrations are still two to three times lower than experimentally measured values. Correctly reproducing dawsonite solubility in standard geochemical simulations requires an as yet undeveloped internally consistent thermodynamic database among dawsonite, gibbsite, boehmite, diaspore, aqueous aluminum complexes and other Al-phases such as albite and kaolinite. These discrepancies question the ability of performance assessment models to correctly predict dawsonite mineralization in a sequestration site. **Citation:** Kaszuba, J. P., H. S. Viswanathan, and J. W. Carey (2011), Relative stability and significance of dawsonite and aluminum minerals in geologic carbon sequestration, *Geophys. Res. Lett.*, 38, L08404, doi:10.1029/2011GL046845.

1. Introduction

[2] Storage of anthropogenic CO_2 in saline aquifers, depleted oil and gas reservoirs, and unmineable coal seams

is one of several strategies targeting the problem of global climate change. The paradigm of CO_2 storage revolves around an idealized progression wherein geochemical trapping mechanisms follow physical trapping [Benson and Cook, 2005]. Geochemical mechanisms for CO_2 trapping (solubility, ionic, and mineral trapping) possess greater long-term stability than physical trapping mechanisms (structural, stratigraphic, capillary, and hydrodynamic trapping) because CO_2 no longer exists as a separate mobile phase within the fluid-rock system. Of these trapping mechanisms, mineral trapping is considered the most secure mechanism for carbon storage in geologic systems because of the relative permanence of minerals. However, mineral trapping occurs at reaction rates on the scale of thousands of years or longer. These rates are the slowest of any of the trapping mechanisms, placing mineral trapping last in the progression. The ultimate fate of CO_2 hinges on the significance of mineral trapping (thousands of years and longer), yet the science of CO_2 sequestration cannot yet predict with any certainty which mineral traps will form.

[3] Dawsonite, $\text{NaAlCO}_3(\text{OH})_2$, is considered a promising phase for long-term mineral sequestration of CO_2 . It could form from common aluminosilicates (alkali feldspar, muscovite, and kaolinite) and Na-bearing brines that do not precipitate typical Ca-, Mg-, and Fe-bearing carbonate minerals, potentially increasing the total mass of carbonate minerals and consequently the storage capacity of a carbon repository. Although modeling studies predict dawsonite formation in carbon repositories [Johnson *et al.*, 2001; Xu *et al.*, 2004; Knauss *et al.*, 2005; Zerai *et al.*, 2006; Xu *et al.*, 2007] and in enhanced oil recovery projects using CO_2 [Cantucci *et al.*, 2009], dawsonite rarely occurs in natural CO_2 fields [Pearce *et al.*, 1996; Klusman, 2003; Wilkinson *et al.*, 2009] and does not appear in laboratory experiments emulating conditions in a carbon repository [Pearce *et al.*, 1996; Kaszuba *et al.*, 2003, 2005; Newell *et al.*, 2008; Hangx and Spiers, 2009]. This discrepancy fuels debate regarding the importance of dawsonite to carbon capture and storage [Hellevang *et al.*, 2005; Bénézeth *et al.*, 2007; Wilkinson *et al.*, 2009; Hellevang *et al.*, 2010]. Resolving this discrepancy is important to determining the significance of dawsonite mineralization to the long-term security of geologic carbon sequestration. For example, mineralization calculations based on geochemical simulations are a crucial component of performance/risk assessment models that evaluate the long term fate of CO_2 [Viswanathan *et al.*, 2008].

[4] The purpose of this paper is to begin to evaluate the underlying causes for inconsistencies between predicted and observed dawsonite stability. We use the controlled conditions of a geochemical laboratory experiment to evaluate dawsonite stability and reactivity. We compare these

¹Department of Geology and Geophysics and School of Energy Resources, University of Wyoming, Laramie, Wyoming, USA.

²Earth and Environmental Sciences Division, Los Alamos National Laboratory, Los Alamos, New Mexico, USA.

Table 1. Water Chemistry as a Function of Time in Dawsonite-Fluid Experiment, 50 and 75°C, 20 MPa

Elapsed Time (h)	P (MPa)	T (°C)	Total Al ^a (uM)	Total Na ^b (mM)	Total C ^c (as mM CO ₂)	Bench pH ^d	In-Situ pH ^e	Comment
—	0.1	25	0	50	50	—	—	solution as synthesized ^f
0.0	0.1	25	0.185	51	47.7	8.89	—	analysis of starting solution
257.8	19.6	50	27.80	51	49.9	8.54	8.42	
348.7	20.2	50	28.24	51	49.0	8.54	8.42	
449.2	19.8	50	19.52	51	49.7	8.56	8.44	
55.9	19.2	75	88.51	51	50.6	8.57	8.41	
149.7	20.2	75	62.98	52	53.2	8.55	8.39	
295.1	20.2	75	59.30	50	NA ^g	NA	NA	filtered with 0.45 μm filter
295.1	20.2	75	63.94	52	NA	8.48	8.33	
297.3	0.1	24	56.52	49	NA	NA	NA	quench sample, filtered with 0.45 μm filter
297.3	0.1	24	99.30	50	NA	8.58	—	quench sample, unfiltered
297.3	0.1	24	68.16	50	NA	NA	NA	quench sample, residual fluid in reaction cell
maximum 2σ uncertainty ^h	—	—	2%	2.6%	5%	0.1	0.1	

^aAqueous aluminum determined by inductively-coupled plasma optical emission spectroscopy (ICP-OES).

^bAqueous sodium determined by ICP mass spectroscopy (ICP-MS).

^cInorganic carbon (as CO₂) determined by coulometric titration [Huffmann, 1977].

^dThe pH measured in sample cooled to 25°C as determined by a Ross microelectrode.

^eIn-situ pH calculated using Geochemist's Workbench 8.0.8 [Bethke and Yeakel, 2009], the thermodynamic dataset thermo.dat, and the b-dot ion association model. Chemical analysis and bench pH at 25°C are used as input data, then temperature is increased to 50 or 75°C as appropriate.

^fSolution used in experiment, synthesized as 0.05 M NaHCO₃.

^gNA, not analyzed.

^hUncertainty as reported by analytical method. Higher analytical (2σ) uncertainties exist for Al in starting solution (12.0%), Al in sample collected at 449.2 hours (10.2%), and Na in sample collected at 348.7 hours (4.8%).

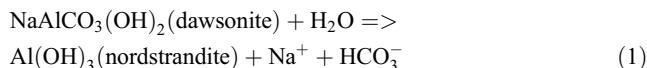
experimental results, and published results for dawsonite solubility, against predictions for dawsonite mineralization produced by an off-the-shelf geochemical code of a type routinely used for modeling carbon sequestration scenarios. From this analysis we demonstrate how geochemical simulations of dawsonite mineralization in a carbon repository may go astray.

2. Reactivity of Dawsonite

[5] A mono-mineralic hydrothermal experiment was performed to examine dawsonite reactivity at two relevant reservoir temperatures. The experiment emulates the later stages of a carbon sequestration scenario in which supercritical CO₂ has already reacted with brine to precipitate dawsonite and is no longer part of the reactive system. Using established experimental methods [Kaszuba et al., 2003, 2005], 237.4 grams of 0.05 molal (M) NaHCO₃ aqueous solution and 2.02 grams of synthetic dawsonite were reacted for 18.7 days (449.2 hours) at 50°C, 20 MPa confining pressure in a rocker bomb. The temperature was then increased to 75°C and the experiment continued for an additional 12.3 days (295.1 hours). Synthetic dawsonite was prepared using methods described by Carey et al. [2006]. Aqueous solution was periodically sampled from the ongoing reaction during the course of the experiment whereas solids and quenched fluid were analyzed after the experiment was completed. Analytical results for fluid samples suggest that the brine achieved an approximate steady state, controlled by the alteration mineral assemblage (Table 1 and Figure 1).

[6] Greater than 95% of the original mass of dawsonite persisted in the experiment as determined by X-ray diffraction analysis of post-reaction solids. Incongruent dissolution of dawsonite yielded Al(OH)₃ polymorphs, a

mixture of gibbsite and nordstrandite (Figure S1 of the auxiliary material).¹ This alteration assemblage is consistent with natural occurrences of co-existing dawsonite and Al(OH)₃ polymorphs [Goldbery and Loughnan, 1970, 1977]:



[7] Geochemical simulations were performed to evaluate how well theoretical predictions capture the actual behavior of dawsonite in the experiments. Predictive geochemical simulations were performed using Geochemist's Workbench 8.0.8 [Bethke and Yeakel, 2009], a geochemical code used to model carbon sequestration scenarios. Simulations used the b-dot ion association model and compared two thermodynamic databases resident in the code, thermo.com.V8.R6⁺ and thermo.dat. Thermo.com.V8.R6⁺ is tacitly accepted by geochemical modelers as a comprehensive data compilation for minerals and aqueous complexes. Thermo.dat is a less comprehensive but internally consistent database. Key reactions and equilibrium constants for these two databases are tabulated in Tables S1 and S2. (Standard log K values for gibbsite, boehmite, diasporite, and corundum in thermo.com.V8.R6⁺ are incorrect for temperatures other than 25°C. Corrected values and an explanation are presented in Table S1.) Dawsonite, gibbsite, and the AlOOH polymorphs boehmite and diasporite were the only aluminum oxyhydroxide minerals considered in our simulations. We did not include nordstrandite or other aluminum hydroxides in the simulations because of the conflicting thermodynamic data reported for these minerals [Anovitz et al., 1991; Hemingway and Sposito, 1996; Tagirov and Schott, 2001]. Total aqueous

¹Auxiliary materials are available in the HTML. doi:10.1029/2011GL046845.

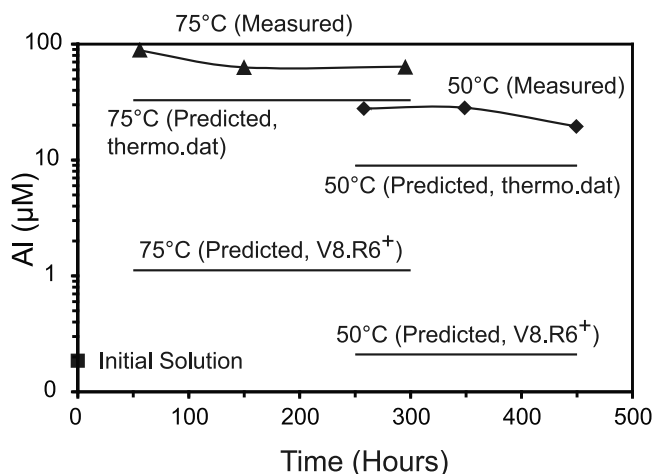


Figure 1. Analytical results for aqueous aluminum plotted as a function of time in a hydrothermal experiment conducted in two stages. Also plotted are predicted values for total dissolved aluminum in both stages of the experiment. The predictions were made using Geochemist's Workbench 8.0.8 and two thermodynamic databases resident in the code (thermo.com.V8.R6⁺ and thermo.dat). The amount of aluminum measured in the experiment is roughly two orders-of-magnitude greater than values predicted using thermo.com.V8.R6⁺, suggesting that dawsonite is less stable than portrayed by calculations using this database. In contrast, geochemical simulations using thermo.dat yield a much improved fit between experiment and simulation.

aluminum predicted by the simulations are compared with experimental data in Figure 1 (aqueous speciation, mineral saturation indices and separate calculations using experimentally generated data to calculate *in-situ* pH (Table 1) are tabulated in Tables S3 and S4).

[8] Simulations using thermo.com.V8.R6⁺ predicted a dawsonite-diaspore assemblage with 0.21 and 1.12 $\mu\text{M/kg}$ total dissolved aluminum at 50 and 75°C, respectively (Figure 1). Dissolved aluminum measured in the experiment is roughly two orders-of-magnitude greater than these predicted values (Table 1 and Figure 1). Higher aqueous aluminum concentrations in the experiment suggest that dawsonite or diaspore is less stable than predicted using thermo.com.V8.R6⁺ (replacing diaspore by gibbsite only improves the prediction by a factor of 4–6). Discrepancies between aluminum concentrations measured in experiments and predicted by geochemical simulations have been observed elsewhere [Carey *et al.*, 2006]. In contrast, geochemical simulations using thermo.dat predicted assemblages of dawsonite and dawsonite-gibbsite with 8.8 and 32.2 $\mu\text{M/kg}$ dissolved aluminum at 50 and 75°C, respectively (Figure 1). While these predictions are roughly two to three times less than experimental values, they represent a much improved match between experiment and calculation compared to simulations using thermo.com.V8.R6⁺.

[9] Recently-published dawsonite solubility measurements [Bénézech *et al.*, 2007] provide a second, independent laboratory dataset to test predictive geochemical simulations for dawsonite mineralization. We simulated their laboratory measurements (Table S5) that were performed at the same temperatures as our experiments (50 and 75°C, Run #8 of

Bénézech *et al.* [2007]). Simulations using thermo.com.V8.R6⁺ predicted dissolved aluminum approximately one order-of-magnitude less than measured values whereas simulations using thermo.dat predicted dissolved aluminum within 10 to 40% of measured values. The simulation using thermo.com.V8.R6⁺ incorrectly predicted formation of diaspore. The simulation using thermo.dat predicted near saturation of gibbsite at 50°C and formation of gibbsite at 75°C whereas bayerite formed in these solubility experiments. Since the solubility of bayerite and gibbsite in sodium chloride solutions is assumed to be the same [Bénézech *et al.*, 2007] we interpret the results of our simulations with thermo.dat as being correct. These computational results are consistent with simulations of our experiments despite differences in the methods employed in the two studies. These differences include solution pH (9.3 to 9.8 versus 8.5 in our study) and ionic strength (1 M versus 50 mM), type of experimental apparatus (in-situ hydrogen-electrode concentration cell versus rocker bomb containing flexible gold reaction cell), pH measurement technique (in-situ versus ex-situ), and pressure of the experiments (0.1 versus 20 MPa).

[10] Geochemical simulations can produce erroneous results by using inaccurate thermodynamic [Oelkers *et al.*, 2009] or kinetic data. In the case of dawsonite, thermodynamic data are well constrained [Ferrante *et al.*, 1976] and have been independently verified [Bénézech *et al.*, 2007]. Values of equilibrium constants for dawsonite (Table S2) are close for both databases. Limited kinetic data are available for dawsonite. One set of dissolution experiments suggests that dawsonite stabilizes at high CO₂ pressure and dissolves relatively quickly after CO₂ pressure diminishes [Hellevang *et al.*, 2005]. However, dawsonite is generally absent from naturally occurring CO₂ fields in which high CO₂ pressures have existed for geologically significant time [Wilkinson *et al.*, 2009].

[11] Equilibrium constants compiled for the hydrolysis of aluminum and for aluminum oxyhydroxide minerals are the likely source of error between the two databases. Thermodynamic data for the hydrolysis of aluminum that is used in the database thermo.com.V8.R6⁺ [Pokrovskii and Helgeson, 1995] and in other geochemical simulations [Shock *et al.*, 1997] contains inconsistencies that increase with temperature [Tagirov and Schott, 2001]. The relative stability of the aluminum oxyhydroxide minerals boehmite and diaspore is significantly different (1.7 to 2.0 log units, Table S2) depending on the choice of thermodynamic data. Results from more recent boehmite solubility measurements [Castet *et al.*, 1993; Bénézech *et al.*, 1997, 2001; Palmer *et al.*, 2001] are the most reliable [Tagirov and Schott, 2001] but are not widely employed.

[12] The database thermo.com.V8.R6⁺ compiles thermodynamic data for gibbsite, boehmite, and diaspore from the work of Pokrovskii and Helgeson [1995]. Simulations using this database incorrectly predict the formation of diaspore instead of gibbsite in our experiments and in the 50 and 75°C experiments of Bénézech *et al.* [2007]. These simulations also predict the relative stability of aluminum oxyhydroxide minerals as diaspore > boehmite > gibbsite (Tables S3 and S4). However, gibbsite is known to be more stable than boehmite at temperatures less than 80°C [Tagirov and Schott, 2001]. In contrast, simulations using thermo.dat correctly predict both formation of gibbsite in the two

experimental studies and the relative stability of the gibbsite as greater than boehmite at these experimental conditions.

[13] Finally, large, extensive thermodynamic databases used in geochemical codes, such as thermo.com.V8.R6⁺, compile thermodynamic data from several different published sources that have used a variety of different laboratory methods. The emergent aqueous model computed with these databases may not be consistent with the original aqueous data [Parkhurst and Appelo, 1999; van der Lee and Lomenech, 2004; Oelkers et al., 2009]. In the case of the database thermo.com.V8.R6⁺, thermodynamic data for minerals and aqueous complexes in the system Al-H₂O is from one source [Pokrovskii and Helgeson, 1995] while thermodynamic data for HCO₃⁻ and Na-bearing aluminum complexes is from a second [Wagman et al., 1982]. Both of these sources are themselves compilations of critically-assessed data.

3. Dawsonite Mineralization in Geologic Carbon Sequestration

[14] Computer simulations most often predict calcite, siderite, ankerite, magnesite, dolomite, and dawsonite as the mineral traps that will form in a carbon repository [Johnson et al., 2001; Xu et al., 2004; Knauss et al., 2005; Zerai et al., 2006; Xu et al., 2007]. The specific minerals and relative amounts that form depend on parameters that include brine chemistry and rock type. However, experiments that emulate a carbon sequestration scenario form siderite, magnesite, and/or calcite, not dawsonite [Kaszuba et al., 2003, 2005; Palandri et al., 2005; Daval et al., 2009; Ketzer et al., 2009; Montes-Hernandez and Pironon, 2009]. Natural CO₂ fields in which supercritical CO₂, aqueous fluid, and rock co-exist contain little [Wilkinson et al., 2009] or no dawsonite [Pearce et al., 1996; Klusman, 2003]. Abundant dawsonite is associated with rather exceptional geochemical environments, most notably in oil shale of the Green River Formation [Smith and Milton, 1966] and in siliciclastic sedimentary rocks permeated by magmatic CO₂ [Baker et al., 1995; Gao et al., 2009].

[15] In this study, we restricted experiments and predictive simulations to an equilibrium-based evaluation of a well-constrained, simple fluid-mineral system in order to focus on dawsonite. The extent to which model predictions emulate dawsonite solubility in these experiments depends on the interactions among aluminum oxyhydroxide minerals and aqueous complexes that compete with dawsonite to constrain aluminum solubility. The latest modeling studies that incorporate updated aluminum thermodynamic data [Gaus et al., 2008; Cantucci et al., 2009] predict dawsonite mineralization will be important in a carbon repository. Our results are directly applicable to the interpretation of dawsonite stability based on chemical analyses of natural and experimental waters. In these cases, it is clear that the size of the dawsonite stability field can be overestimated by the choice of thermodynamic data. However, while this is a piece of the dawsonite puzzle, these results do not challenge the thermodynamic stability of dawsonite at high CO₂ pressure [e.g., Bénézech et al., 2007]. Thus, in addition to the thermodynamic constraints employed in this study, additional factors must influence dawsonite reactivity. These include complexities inherent in kinetic processes and in multi-mineral multi-component brine-rock interactions

characteristic of natural systems. In particular, the potential influence of multi-phase (H₂O + supercritical CO₂) fluids on the stability of dawsonite relative to aluminosilicate minerals prevalent in natural systems may be important.

[16] Our results demonstrate the challenges in developing a realistic model for CO₂ mineralization in a carbon repository over long time scales, thousands of years and longer. If performance assessment models could accurately predict mineralization, uncertainty in CO₂ migration could be greatly reduced. However, our results bring into question the extent to which performance assessment models can accurately predict dawsonite mineralization when assessing a sequestration site. Confidence in these models can increase by improving the internal consistency of thermodynamic databases through relevant field and laboratory experiments that assess the thermodynamic properties of critical phases and the computer codes that simulate geologic carbon sequestration.

[17] **Acknowledgments.** We acknowledge Thomas Carpenter for his able assistance in the hydrothermal lab, Ren Guan for dawsonite synthesis and XRD analysis, and Dale Counce for aqueous analyses. T. Meuzelaar and G. Thyne reviewed an earlier version of this paper. Laboratory work was funded by the LDRD program of Los Alamos National Laboratory. J. P. Kaszuba's work in data analysis and manuscript preparation was supported by the UW School of Energy Resources.

[18] The Editor thanks two anonymous reviewers for their assistance in evaluating this paper.

References

- Anovitz, L. M., D. Perkins, and E. J. Essene (1991), Metastability in near-surface rocks of minerals in the system Al₂O₃-SiO₂-H₂O, *Clays Clay Miner.*, 39, 225–233, doi:10.1346/CCMN.1991.0390301.
- Baker, J. C., G. P. Bai, P. J. Hamilton, S. D. Golding, and J. B. Keene (1995), Continental-scale magmatic carbon dioxide seepage recorded by dawsonite in the Bowen Gunnedah-Sydney basin system, Eastern Australia, *J. Sediment. Res.*, A65, 522–530.
- Bénézech, P., D. A. Palmer, and D. J. Wesolowski (1997), The aqueous chemistry of aluminum: A new approach to high-temperature solubility measurements, *Geothermics*, 26, 465–481, doi:10.1016/S0375-6505(97)00006-0.
- Bénézech, P., D. A. Palmer, and D. J. Wesolowski (2001), Aqueous high-temperature solubility studies. II: The solubility of boehmite at 0.03 m ionic strength as a function of temperature and pH as determined by in situ measurements, *Geochim. Cosmochim. Acta*, 65, 2097–2111, doi:10.1016/S0016-7037(01)00585-3.
- Bénézech, P., D. A. Palmer, L. M. Anovitz, and J. Horita (2007), Dawsonite synthesis and reevaluation of its thermodynamic properties from solubility measurements: Implications for mineral trapping of CO₂, *Geochim. Cosmochim. Acta*, 71, 4438–4455, doi:10.1016/j.gca.2007.07.003.
- Benson, S., and P. Cook (2005), Underground geological storage, in *IPCC Special Report on Carbon Dioxide Capture and Storage*, edited by B. Metz et al., pp. 195–276, Cambridge Univ. Press, Cambridge, U. K.
- Bethke, C. M., and S. Yeakel (2009), *The Geochemist's Workbench Release 8.0: Reaction Modeling Guide*, 84 pp., Univ. of Ill., Champaign.
- Cantucci, B., G. Montegrossi, O. Vaselli, F. Tassi, F. Quattrocchi, and E. H. Perkins (2009), Geochemical modeling of CO₂ storage in deep reservoirs: The Weyburn Project (Canada) case study, *Chem. Geol.*, 265, 181–197, doi:10.1016/j.chemgeo.2008.12.029.
- Carey, J. W., R.-G. Duan, and J. P. Kaszuba (2006), Crystal chemistry and reactivity of dawsonite, paper presented at GHGT-8, 8th International Conference on Greenhouse Gas Control Technologies, Elsevier Sci., Trondheim, Norway.
- Castet, S., J. L. Dandurand, J. Schott, and R. Gout (1993), Boehmite solubility and aqueous aluminum speciation in hydrothermal solutions (90–350°C): Experimental study and modeling, *Geochim. Cosmochim. Acta*, 57, 4869–4884, doi:10.1016/0016-7037(93)90126-H.
- Daval, D., I. Martinez, J. Corvisier, N. Findling, B. Goffé, and F. Guyot (2009), Carbonation of Ca-bearing silicates, the case of wollastonite: Experimental investigations and kinetic modeling, *Chem. Geol.*, 265, 63–78, doi:10.1016/j.chemgeo.2009.01.022.

- Ferrante, M. J., J. M. Stuve, and D. W. Richardson (1976), Thermodynamic data for synthetic dawsonite, *Rep. of Invest.*, 8129, 13 pp., U.S. Bur. of Mines, Washington, D. C.
- Gao, Y. Q., L. Liu, and W. X. Hu (2009), Petrology and isotopic geochemistry of dawsonite-bearing sandstones in Hailaer basin, northeastern China, *Appl. Geochem.*, 24, 1724–1738, doi:10.1016/j.apgeochem.2009.05.002.
- Gaus, I., P. Audigane, L. Andre, J. Lions, N. Jacquemet, P. Dutst, I. Czernichowski-Lauriol, and M. Azaroual (2008), Geochemical and solute transport modelling for CO₂ storage, what to expect from it?, *Int. J. Greenhouse Gas Control*, 2, 605–625, doi:10.1016/j.ijggc.2008.02.011.
- Goldbery, R., and F. C. Loughnan (1970), Dawsonite and nordstrandite in Permian Berry Formation of Sydney Basin, New South Wales, *Am. Mineral.*, 55, 477–490.
- Goldbery, R., and F. C. Loughnan (1977), Dawsonite, alumohydrocalcite, nordstrandite and gorceixite in Permian marine strata of Sydney Basin, Australia, *Sedimentology*, 24, 565–579, doi:10.1111/j.1365-3091.1977.tb00139.x.
- Hangx, S. J. T., and C. J. Spiers (2009), Reaction of plagioclase feldspars with CO₂ under hydrothermal conditions, *Chem. Geol.*, 265, 88–98, doi:10.1016/j.chemgeo.2008.12.005.
- Hellevang, H., P. Aagaard, E. H. Oelkers, and B. Kvamme (2005), Can dawsonite permanently trap CO₂?, *Environ. Sci. Technol.*, 39, 8281–8287, doi:10.1021/es0504791.
- Hellevang, H., J. Declercq, B. Kvamme, and P. Aagaard (2010), The dissolution rates of dawsonite at pH 0.9 to 5 and temperatures of 22, 60 and 77°C, *Appl. Geochem.*, 25, 1575–1586, doi:10.1016/j.apgeochem.2010.08.007.
- Hemingway, B. S., and G. Sposito (1996), Inorganic aluminium-bearing solid phases, in *The Environmental Chemistry of Aluminium*, edited by G. Sposito, pp. 81–116, CRC Press, Boca Raton, Fla.
- Huffmann, E. (1977), Performance of a new automatic carbon dioxide coulometer, *Microchem. J.*, 22, 567–573.
- Johnson, J. W., J. J. Nitao, C. I. Steefel, and K. G. Knauss (2001), Reactive transport modeling of geologic CO₂ sequestration in saline aquifers: The influence of intra-aquifer shales and the relative effectiveness of structural solubility and mineral trapping during prograde and retrograde sequestration, paper presented at First National Conference on Carbon Sequestration, Natl. Energy Technol. Lab., U.S. Dep. of Energy, Washington, D. C., 14–17 May.
- Kaszuba, J. P., D. R. Janecky, and M. G. Snow (2003), Carbon dioxide reaction processes in a model brine aquifer at 200°C and 200 bars: Implications for geologic sequestration of carbon, *Appl. Geochem.*, 18, 1065–1080, doi:10.1016/S0883-2927(02)00239-1.
- Kaszuba, J. P., D. R. Janecky, and M. G. Snow (2005), Experimental evaluation of mixed fluid reactions between supercritical carbon dioxide and NaCl brine: Relevance to the integrity of a geologic carbon repository, *Chem. Geol.*, 217, 277–293, doi:10.1016/j.chemgeo.2004.12.014.
- Ketzer, J. M., R. Iglesias, S. Einloft, J. Dullius, R. Ligabue, and V. de Lima (2009), Water-rock-CO₂ interactions in saline aquifers aimed for carbon dioxide storage: Experimental and numerical modeling studies of the Rio Bonito Formation (Permian), southern Brazil, *Appl. Geochem.*, 24, 760–767, doi:10.1016/j.apgeochem.2009.01.001.
- Klusman, R. W. (2003), A geochemical perspective and assessment of leakage potential for a mature carbon dioxide-enhanced oil recovery project and as a prototype for carbon dioxide sequestration; Rangely field, Colorado, *AAPG Bull.*, 87, 1485–1507, doi:10.1306/04220302032.
- Knauss, K. G., J. W. Johnson, and C. I. Steefel (2005), Evaluation of the impact of CO₂, co-contaminant gas, aqueous fluid and reservoir rock interactions on the geologic sequestration of CO₂, *Chem. Geol.*, 217, 339–350, doi:10.1016/j.chemgeo.2004.12.017.
- Montes-Hernandez, G., and J. Pironon (2009), Hematite and iron carbonate precipitation-coexistence at the iron-montmorillonite-salt solution-CO₂ interfaces under high gas pressure at 150°C, *Appl. Clay Sci.*, 45, 194–200, doi:10.1016/j.clay.2009.06.004.
- Newell, D. L., J. P. Kaszuba, H. S. Viswanathan, R. J. Pawar, and T. Carpenter (2008), Significance of carbonate buffers in natural waters reacting with supercritical CO₂: Implications for monitoring, measuring and verification (MMV) of geologic carbon sequestration, *Geophys. Res. Lett.*, 35, L23403, doi:10.1029/2008GL035615.
- Oelkers, E. H., P. Bénézech, and G. S. Pokrovski (2009), Thermodynamic databases for water-rock interaction, in *Thermodynamics and Kinetics of Water-Rock Interaction*, edited by E. H. Oelkers and J. Schott, pp. 1–46, Mineral. Soc. Am., Chantilly, Va.
- Palandri, J. L., R. J. Rosenbauer, and Y. K. Kharaka (2005), Ferric iron in sediments as a novel CO₂ mineral trap: CO₂-SO₂ reaction with hematite, *Appl. Geochem.*, 20, 2038–2048, doi:10.1016/j.apgeochem.2005.06.005.
- Palmer, D. A., P. Bénézech, and D. J. Wesolowski (2001), Aqueous high-temperature solubility studies. I. The solubility of boehmite as functions of ionic strength (to 5 molal, NaCl), temperature (100–290°C), and pH as determined by in situ measurements, *Geochim. Cosmochim. Acta*, 65, 2081–2095, doi:10.1016/S0016-7037(01)00584-1.
- Parkhurst, D. L., and C. A. J. Appelo (1999), User's guide to PHREEQC (v. 2): A computer program for speciation, batch-reaction, one-dimensional transport, and inverse geochemical calculations, *U.S. Geol. Surv. Water Resour. Invest. Rep.*, WRI 99-4259, 312 pp.
- Pearce, J. M., S. Holloway, H. Wacker, M. K. Nelis, C. Rochelle, and K. Bateman (1996), Natural occurrences as analogues for the geological disposal of carbon dioxide, *Energy Convers. Manage.*, 37, 1123–1128, doi:10.1016/0196-8904(95)00309-6.
- Pokrovskii, V. A., and H. C. Helgeson (1995), Thermodynamic properties of aqueous species and the solubilities of minerals at high pressures and temperatures: The system Al₂O₃-H₂O-NaCl, *Am. J. Sci.*, 295, 1255–1342, doi:10.2475/ajs.295.10.1255.
- Shock, E. L., D. C. Sassani, M. Willis, and D. A. Sverjensky (1997), Inorganic species in geologic fluids: Correlations among standard molal thermodynamic properties of aqueous ions and hydroxide complexes, *Geochim. Cosmochim. Acta*, 61, 907–950, doi:10.1016/S0016-7037(96)00339-0.
- Smith, J. W., and C. Milton (1966), Dawsonite in the Green River Formation of Colorado, *Econ. Geol.*, 61, 1029–1042, doi:10.2113/gsecongeo.61.6.1029.
- Tagirov, B., and J. Schott (2001), Aluminum speciation in crustal fluids revisited, *Geochim. Cosmochim. Acta*, 65, 3965–3992, doi:10.1016/S0016-7037(01)00705-0.
- van der Lee, J., and C. Lomenech (2004), Towards a common thermodynamic database for speciation models, *Radiochim. Acta*, 92, 811–818, doi:10.1524/ract.92.9.811.54998.
- Viswanathan, H. S., R. J. Pawar, P. H. Stauffer, J. P. Kaszuba, J. W. Carey, S. C. Olsen, G. N. Keating, D. Kavetski, and G. D. Guthrie (2008), Development of a hybrid process and system model for the assessment of wellbore leakage at a geologic CO₂ sequestration site, *Environ. Sci. Technol.*, 42, 7280–7286, doi:10.1021/es800417x.
- Wagman, D. D., W. H. Evans, V. B. Parker, R. H. Schumm, I. Halow, S. M. Bailey, K. L. Churney, and R. L. Nuttall (1982), The NBS tables of chemical thermodynamic properties - Selected values for inorganic and C1 and C2 organic substances in SI units, report, 392 pp., Am. Chem. Soc., Washington, D. C.
- Wilkinson, M., R. S. Haszeldine, A. E. Fallick, N. Odling, S. J. Stoker, and R. W. Gatliff (2009), CO₂-mineral reaction in a natural analogue for CO₂ storage: Implications for modeling, *J. Sediment. Res.*, 79, 486–494, doi:10.2110/jsr.2009.052.
- Xu, T. F., J. A. Apps, and K. Pruess (2004), Numerical simulation of CO₂ disposal by mineral trapping in deep aquifers, *Appl. Geochem.*, 19, 917–936, doi:10.1016/j.apgeochem.2003.11.003.
- Xu, T. F., J. A. Apps, K. Pruess, and H. Yamamoto (2007), Numerical modeling of injection and mineral trapping of CO₂ with H₂S and SO₂ in a sandstone formation, *Chem. Geol.*, 242, 319–346, doi:10.1016/j.chemgeo.2007.03.022.
- Zerai, B., B. Z. Saylor, and G. Matisoff (2006), Computer simulation of CO₂ trapped through mineral precipitation in the Rose Run Sandstone, Ohio, *Appl. Geochem.*, 21, 223–240, doi:10.1016/j.apgeochem.2005.11.002.

J. W. Carey and H. S. Viswanathan, Earth and Environmental Sciences Division, Los Alamos National Laboratory, PO Box 1663, Los Alamos, NM 87545, USA.

J. P. Kaszuba, Department of Geology and Geophysics and School of Energy Resources, University of Wyoming, Laramie, WY 82071, USA.

Auxiliary material for Paper 2011GL046845

Relative stability and significance of dawsonite and aluminum minerals in geologic carbon sequestration

John P. Kaszuba

Department of Geology and Geophysics and School of Energy Resources, University of Wyoming, Laramie, Wyoming, USA

Hari S. Viswanathan and J. William Carey

Earth and Environmental Sciences Division, Los Alamos National Laboratory, Los Alamos, New Mexico, USA

Kaszuba, J. P., H. S. Viswanathan, and J. W. Carey (2011), Relative stability and significance of dawsonite and aluminum minerals in geologic

Introduction

This data set contains equilibrium constants of gibbsite, boehmite, diaspore, and corundum used in geochemical simulations as well as tabula

Original and corrected values for equilibrium constants of gibbsite, boehmite, diaspore, and corundum for the thermo.com.V8.R6+ database, al

1. 2011gl046845-ts01.pdf

Original and corrected values for equilibrium constants of gibbsite, boehmite, diaspore, and corundum for the thermo.com.V8.R6+ database.

2. 2011gl046845-ts02.pdf

Equilibrium constants at experimental temperatures for dawsonite and other minerals as well as aqueous species of direct relevance.

3. 2011gl046845-ts03.pdf

Summary of results for predictive geochemical simulations.

4. 2011gl046845-ts04.pdf

Results for calculation of in-situ pH of fluid at 50 and 75°C based on experimental fluid composition data (Table 1). Also tabulated is a s

5. 2011gl046845-ts05.pdf

Summary of results for predictive geochemical simulations, 50 and 75°C experiments in Benezeth et al. [2007].

6. 2011gl046845-fs01.eps

X-ray diffraction results for dawsonite used in the experiment and for solids recovered after the experiment was completed.

References

Benezeth, P., Palmer, D.A., Anovitz, L.M., and Horita, J., 2007, Dawsonite synthesis and reevaluation of its thermodynamic properties from s

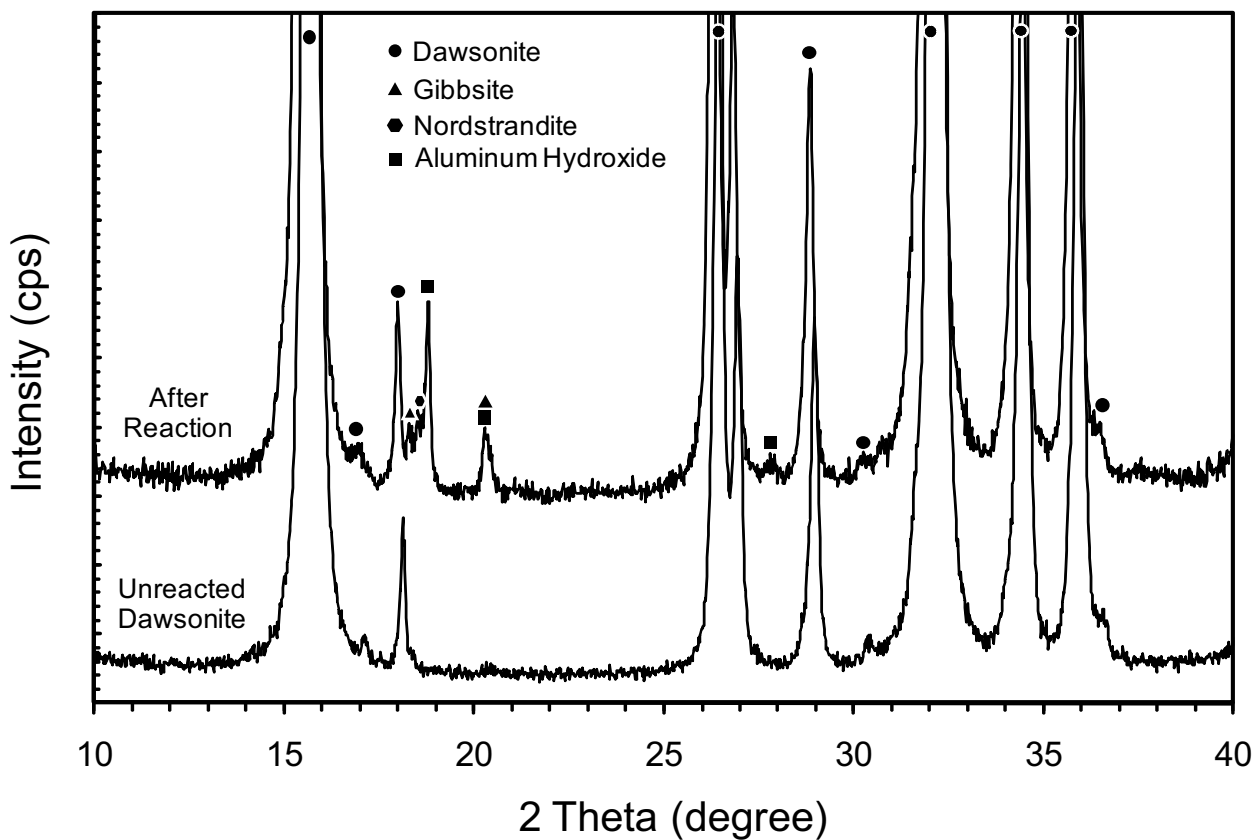


Figure S1. X-ray diffraction results for dawsonite used in the experiment and for solids recovered after the experiment was completed.

1 Table S1. Original and corrected values for equilibrium constants of gibbsite, boehmite, diaspore, and corundum for
 2 thermo.com.V8.R6⁺.

3

Temperature (°C)	Log K							
	Original Values in thermo.com.V8.R6 ⁺				Corrected Values			
	Gibbsite	Boehmite	Diaspore	Corundum	Gibbsite	Boehmite	Diaspore	Corundum
0	9.3787	9.3656	8.9174	22.3407	9.402	9.369	8.919	22.425
25	7.560	7.5642	7.1603	18.3121	7.756	7.564	7.16	18.312
60	5.8286	5.465	5.1159	13.3851	5.865	5.469	5.118	13.519
100	3.9979	3.5242	3.2294	8.5405	4.142	3.54	3.237	9.082
150	2.0853	1.5677	1.3302	3.3044	2.428	1.6	1.346	4.604
200	0.4377	-0.0516	-0.2409	-1.3281	1.02	-0.003	-0.219	0.899
250	-1.0575	-1.4697	-1.618	-5.5872	-0.217	-1.408	-1.593	-2.333
300	-2.4754	-2.7773	-2.8906	-9.6296	-1.368	-2.705	-2.865	-5.293

4
 5 Note: Standard log K values for gibbsite, boehmite, diaspore, and corundum in the thermo.com.V8.R6⁺ database are incorrect for
 6 temperatures different than 25°C. This is due to an error in heat capacity values, for these four phases only, which were used in the
 7 original construction of thermo.com.V8.R6⁺. We confirmed these findings with James Johnson, author of SUPCRT (Johnson, J. W.,
 8 E. H. Oelkers, and H. C. Helgeson (1992), SUPCRT92: A software package for calculating the standard molal thermodynamic
 9 properties of minerals, gases, aqueous species, and reactions from 1 to 5000 bar and 0 to 1000°C, *Comput. Geosci.*, 18, 899-947) and
 10 one of the original compilers of the thermo.com.V8.R6⁺ database, also known as the Lawrence Livermore National Laboratory
 11 (LLNL) combined database. We corrected log K values for gibbsite, boehmite, diaspore, and corundum by running SUPCRT96 with
 12 the sprons96.dat database, which is fully consistent with the original intention of thermo.com.V8.R6⁺. The differences between the
 13 original and corrected log K values for boehmite and diaspore are quite small while the difference for gibbsite is more significant and
 14 corundum is corrected by a substantial degree. The geochemical simulations described in this paper employ these corrected log K
 15 values. Since diaspore is the stable aluminum oxyhydroxide mineral in our simulations that use thermo.com.V8.R6⁺, our results and
 16 interpretations do not change by using corrected instead of original log K values.

17

1 Table S2. Equilibrium constants at experimental temperatures for dawsonite and other minerals
 2 as well as aqueous species of direct relevance.

Reaction	thermo.dat		thermo.com.V8.R6 ⁺	
	log K at 50°C	log K at 75°C	log K at 50°C	log K at 75°C
Dawsonite + 3H ⁺ = Na ⁺ + Al ³⁺ + HCO ₃ ⁻ + 2H ₂ O	3.7675	3.0429	3.3182	2.4524
^a Gibbsite + 3H ⁺ = Al ³⁺ + 3H ₂ O	6.6957	5.6419	6.3646	5.1701
Boehmite + 3H ⁺ = Al ³⁺ + 2H ₂ O	8.0024	6.6532	6.0250	4.6940
Diaspore + 3H ⁺ = Al ³⁺ + 2H ₂ O	7.2764	6.0293	5.6598	4.3625
CO ₂ (aq) + H ₂ O = HCO ₃ ⁻ + H ⁺	-6.3221	-6.3433	-6.2690	-6.2865
NaHCO ₃ (aq) = Na ⁺ + HCO ₃ ⁻	0.0594	0.2409	0.0385	0.2241
^b Al(OH) ₄ ⁻ + 4H ⁺ = 4 H ₂ O + Al ³⁺	19.8454	18.2981	---	---
^c AlO ₂ ⁻ + 4H ⁺ = 2H ₂ O + Al ³⁺	---	---	20.4427	18.3583
^b Al(OH) ₃ (aq) + 3H ⁺ = 3H ₂ O + Al ³⁺	14.0532	12.6072	---	---
^c HAIO ₂ (aq) + 3H ⁺ = 2H ₂ O + Al ³⁺	---	---	14.4491	12.7082
^c NaAlO ₂ (aq) + 4H ⁺ = 2H ₂ O + Al ³⁺ + Na ⁺	---	---	21.0338	18.7820
Al(OH) ₂ ⁺ + 2H ⁺ = Al ³⁺ + 2H ₂ O	8.8547	7.9641	9.2419	8.0455

3 ^aWe used corrected log K values in Table A1 to determine equilibrium constants for gibbsite,
 4 boehmite, and diaspore at 50 and 75°C. For comparison, using original log K values from
 5 thermo.com.V8.R6⁺ to determine equilibrium constants for gibbsite, boehmite, and diaspore at
 6 50°C yield 6.3452, 6.0227, and 5.6588, respectively; and at 75°C yield 5.1011, 4.6864, and
 7 4.3587. The differences for boehmite and diaspore are quite small, while the difference for
 8 gibbsite is more significant.

9 ^bthis aqueous species is part of thermo.dat but not thermo.com.V8.R6⁺

10 ^cthis aqueous species is part of thermo.com.V8.R6⁺ but not thermo.dat

11

12

1 Table S3. Summary of results for predictive geochemical simulations.

Aqueous Species	50°C				75°C			
	thermo.dat		thermo.com.V8.R6 ⁺		thermo.dat		thermo.com.V8.R6 ⁺	
	molality	log molality	molality	log molality	molality	log molality	molality	log molality
Na ⁺	4.86E-02	-1.313	8.86E-02	-1.053	6.40E-02	-1.194	1.56E-01	-0.807
NaHCO ₃ (aq)	1.34E-03	-2.873	4.19E-03	-2.377	1.43E-03	-2.846	7.38E-03	-2.132
NaCO ₃ ⁻	2.29E-05	-4.640	5.99E-05	-4.223	1.89E-05	-4.725	7.46E-05	-4.127
NaOH	1.64E-07	-6.785	5.75E-08	-7.241	6.91E-07	-6.161	3.34E-07	-6.476
^a NaAlO ₂ (aq)	---	---	2.83E-09	-8.549	---	---	3.42E-08	-7.466
Total	0.050	-1.301	0.093	-1.032	0.065	-1.184	0.163	-0.787
HCO ₃ ⁻	4.74E-02	-1.325	8.61E-02	-1.065	6.22E-02	-1.206	1.51E-01	-0.822
NaHCO ₃ (aq)	1.34E-03	-2.873	4.19E-03	-2.377	1.43E-03	-2.846	7.38E-03	-2.132
CO ₂ (aq)	6.65E-04	-3.177	1.28E-03	-2.894	9.67E-04	-3.014	2.65E-03	-2.578
CO ₃ ²⁻	6.25E-04	-3.204	1.21E-03	-2.918	8.86E-04	-3.053	2.55E-03	-2.594
NaCO ₃ ⁻	2.29E-05	-4.640	5.99E-05	-4.223	1.89E-05	-4.725	7.46E-05	-4.127
Total	0.050	-1.301	0.093	-1.032	0.065	-1.184	0.163	-0.787
^b Al(OH) ₄ ⁻	8.78E-06	-5.056	---	---	3.23E-05	-4.491	---	---
^a AlO ₂ ⁻	---	---	2.08E-07	-6.683	---	---	1.10E-06	-5.957
^b Al(OH) ₃ (aq)	3.06E-08	-7.514	---	---	1.23E-07	-6.912	---	---
^a HAlO ₂ (aq)	---	---	1.62E-09	-8.791	---	---	4.52E-09	-8.345
^a NaAlO ₂ (aq)	---	---	2.83E-09	-8.549	---	---	3.42E-08	-7.466
Al(OH) ₂ ⁺	5.50E-11	-10.26	3.46E-12	-11.46	5.82E-11	-10.24	3.58E-12	-11.44
Total	8.81E-06	-5.055	2.12E-07	-6.674	3.24E-05	-4.490	1.13E-06	-5.946
pH	8.088		7.988		8.051		7.903	

	Saturation Indices			
dawsonite	0	0	0	0
gibbsite	-0.1086	-0.7048	0	-0.8079
boehmite	-1.415	-0.3651	-1.0117	-0.3319
diaspore	-0.6893	0	-0.3875	0

2 ^athis aqueous species is part of thermo.com.V8.R6⁺ but not thermo.dat

3 ^bthis aqueous species is part of thermo.dat but not thermo.com.V8.R6⁺

1 Table S4. Results for calculation of in-situ pH of fluid at 50 and 75°C based on experimental fluid composition data (Table 1). Also
 2 tabulated is a summary of aqueous speciation, pH, and saturation state of the fluid.

Aqueous Species	50°C at 449.2 hours				75°C at 295.1 hours			
	thermo.dat		thermo.com.V8.R6 ⁺		thermo.dat		thermo.com.V8.R6 ⁺	
	molality	log molality	molality	log molality	molality	log molality	molality	log molality
Na ⁺	4.98E-02	-1.303	4.98E-02	-1.303	5.00E-02	-1.301	5.01E-02	-1.300
NaHCO ₃ (aq)	1.35E-03	-2.869	1.40E-03	-2.853	8.85E-04	-3.053	9.10E-04	-3.041
NaCO ₃ ⁻	5.18E-05	-4.286	4.92E-05	-4.308	2.16E-05	-4.665	1.85E-05	-4.734
^a NaAlO ₂ (aq)	---	---	1.62E-07	-6.790	---	---	7.66E-07	-6.116
NaOH	3.74E-07	-6.427	8.69E-08	-7.061	1.04E-06	-5.984	2.63E-07	-6.581
Total	0.051	-1.291	0.051	-1.290	0.051	-1.293	0.051	-1.292
HCO ₃ ⁻	4.69E-02	-1.329	4.68E-02	-1.330	4.75E-02	-1.323	4.74E-02	-1.325
CO ₃ ²⁻	1.40E-03	-2.855	1.47E-03	-2.832	1.20E-03	-2.920	1.31E-03	-2.883
NaHCO ₃ (aq)	1.35E-03	-2.869	1.40E-03	-2.853	8.85E-04	-3.053	9.10E-04	-3.041
CO ₂ (aq)	2.94E-04	-3.532	2.82E-04	-3.549	3.99E-04	-3.399	4.15E-04	-3.382
NaCO ₃ ⁻	5.18E-05	-4.286	4.92E-05	-4.308	2.16E-05	-4.665	1.85E-05	-4.734
Total	0.050	-1.301	0.050	-1.301	0.050	-1.301	0.050	-1.301
^b Al(OH) ₄ ⁻	1.95E-05	-4.710	---	---	6.38E-05	-4.195	---	---
^a AlO ₂ ⁻	---	---	1.93E-05	-4.714	---	---	6.31E-05	-4.200
^a NaAlO ₂ (aq)	---	---	1.62E-07	-6.790	---	---	7.66E-07	-6.116
^b Al(OH) ₃ (aq)	3.58E-08	-7.446	---	---	1.19E-07	-6.926	---	---
^a HAlO ₂ (aq)	---	---	6.17E-08	-7.210	---	---	1.28E-07	-6.894
Total	1.95E-05	-4.710	1.95E-05	-4.709	6.39E-05	-4.194	6.39E-05	-4.194
pH	8.437		8.398		8.326		8.248	

Saturation Indices

dawsonite	0.0301	1.1073	-0.1739	0.5452
gibbsite	-0.0884	0.8749	0.0394	0.6442
boehmite	-1.3951	1.2146	-0.9719	1.1202
diaspore	-0.6691	1.5798	-0.3481	1.4518

3 ^athis aqueous species is part of thermo.com.V8.R6⁺ but not thermo.dat

4 ^bthis aqueous species is part of thermo.dat but not thermo.com.V8.R6⁺

5

1 Table S5. Summary of results for predictive geochemical simulations, 50 and 75°C experiments in *Bénézeth et al.* [2007].

T°C	time of sampling (hours)	pH			total Al (umolal)		
		measured in-situ	thermo.dat	thermo.com.V8.R6 ⁺	measured	thermo.dat	thermo.com.V8.R6 ⁺
50.1	136	9.802	9.706	9.203	468	442	447
50.2	183	9.757	9.706	9.203	407	442	447
75.1	112	9.309	9.409	8.707	676	874	917
75.2	160	9.282	9.409	8.707	631	874	917

2
3 Table A4. Summary of results for predictive geochemical simulations, 50 and 75°C experiments in *Bénézeth et al.* [2007] (continued).

T°C	time of sampling (hours)	total Na (molal)			total C (molal)		
		measured	thermo.dat	thermo.com.V8.R6 ⁺	measured	thermo.dat	thermo.com.V8.R6 ⁺
50.1	136	1.03	0.997	1.01	12	10.4	22.1
50.2	183	1.01	0.997	1.01	12.7	10.4	22.1
75.1	112	1.18	0.998	1.03	16	11.8	45.4
75.2	160	1.06	0.998	1.03	16.3	11.8	45.4

4
5 Table A4. Summary of results for predictive geochemical simulations, 50 and 75°C experiments in *Bénézeth et al.* [2007] (continued).

T°C	time of sampling (hours)	Mineral assemblage	Saturation index, thermo.dat				Saturation index, thermo.com.V8.R6 ⁺			
			dawsonite	gibbsite	boehmite	diaspore	dawsonite	gibbsite	boehmite	diaspore
50.1	136	dawsonite + bayerite	0	-0.1052	-1.3977	-0.672	0	-0.7179	-0.365	0
50.2	183	dawsonite + bayerite	0	-0.1052	-1.3977	-0.672	0	-0.7179	-0.365	0
75.1	112	dawsonite + bayerite	0	0	-0.998	-0.3738	0	-0.8208	-0.3319	0

75.2	160	dawsonite + bayerite	0	0	-0.998	-0.3738	0	-0.8208	-0.3319	0
------	-----	-------------------------	---	---	--------	---------	---	---------	---------	---

6 ^a*Bénézeth et al.* [2007] assume bayerite solubility = gibbsite solubility

7